ELSEVIER

Journal of Immunological Methods 278 (2003) 305–317

JIM
Journal of Immunological Methods

www.elsevier.com/locate/jim

Computational Modeling

An analysis tool to quantify the efficiency of cell tethering and firm-adhesion in the parallel-plate flow chamber

Yi Zhang, Sriram Neelamegham*

Bioengineering Laboratory, Department of Chemical Engineering, State University of New York at Buffalo, 906 Furnas Hall, Buffalo, NY 14260, USA

Received 15 September 2002; received in revised form 21 December 2002; accepted 4 February 2003

Abstract

The parallel-plate flow chamber is applied in immunological studies to quantify the adhesivity of cells (e.g. leukocytes) onto ligand-bearing substrates (e.g. endothelial cells) under fluid-flow conditions that mimic the human vasculature. It is also applied to quantify platelet adhesion in vascular injury models, and tumor cell adhesion in models of cancer metastasis. Typical measures of cell adhesion in this setup include the rolling and adherent cell density. These measures are functions of not only the cellular adhesivity, but also of the physical features of the experimental system (e.g. inlet cell concentration) and observation time. Here, we present a mathematical model to better analyze experimental data on cell rolling, firm-arrest and transmigration. The overall goal is to quantify the biological adhesivity of cells independent of the physical parameters that control the rate of cell–substrate and cell–cell collision. This analysis yields four independent parameters: *Primary capture frequency* quantifies the rate at which cells in the free stream initiate rolling. *Firm-arrest frequency* is a measure of the transition from rolling to firm-binding. These two frequency parameters are inversely proportional to the distance the average cell convects in the free stream adjacent to the substrate before tethering, or rolls on the substrate before firm-adhesion, respectively. *Rolling-release frequency* is introduced to quantify the reversible release of cells from rolling back into the free stream. Finally, *cell–cell capture probability* quantifies the fraction of collisions between cells in free stream and recruited substrate-bound cells that result in tethering. The proposed analysis methodology may find application in studies of inflammation, thrombosis and cancer research.

Keywords: Leukocyte; Endothelium; Hydrodynamic shear; Adhesion efficiency; Integrin; Selectin

1. Introduction

The parallel-plate flow chamber has a defined flow profile that simulates the features of hydrodynamic forces found in the vasculature. It is commonly used in immunological studies, especially to simulate inflammatory ailments where leukocytes adhere onto the vascular endothelium under flow (Gopalan et al., 1997). It has also been used to study the rate of platelet adhesion and thrombus formation in models of vascular injury (Kroll et al., 1996). Recent studies also quantify the rate of tumor cell attachment to platelets in a model of hematogeneous metastasis (Felding-Habermann et al., 1996). While some of the studies aim to identify the molecules involved in

Abbreviations: θ_{fr}, primary capture frequency; θ_{ra}, firm-arrest frequency; θ_{cc}, cell–cell capture probability; θ_{rf}, rolling-release frequency; PSGL-1, P-selectin glycoprotein ligand-1; ICAM-1, intercellular adhesion molecule-1.

* Corresponding author. Tel.: +1-716-645-2911x2220; fax: +1-716-645-3822.

E-mail address: neel@eng.buffalo.edu (S. Neelamegham).

0022-1759/03/$ - see front matter © 2003 Elsevier Science B.V. All rights reserved.
doi:10.1016/S0022-1759(03)00082-6

cell adhesion under shear conditions, others quantify the biophysics of receptor–ligand interaction (Alon et al., 1995). The emphasis of the latter work is on understanding the structure–function relationships guiding adhesion molecule affinities upon application of mechanical forces. Overall, this device is commonly applied in studies of various families of cell-surface adhesion molecules including members of the selectin, integrin and immunoglobulin families.

Three parameters, the density of rolling cells, the density of adherent cells and the time for cell transmigration or diapedesis, are quantified in typical flow chamber experiments. While these parameters are measures of the biological properties of cells/adhesion molecules, they are also dependent on the physical features of the system that control the rate of cell collision with the ligand-bearing substrate and with surface-bound cells. These physical features include the cell and fluid density, cell size, flow chamber size and applied shear rate (Munn et al., 1994; Zhang and Neelamegham, 2002). Further, the number of rolling cells directly influences the number of adherent cells, which in turn alters the rate of cell transmigration. Since the aim of flow chamber studies is to quantify the adhesivity of cells and receptors over a range of fluid shear conditions independent of the physical features of the flow system, we recently proposed an analysis strategy to quantify the biological adhesivity of cells (Zhang and Neelamegham, 2002).

In the current manuscript, we present a major simplification of our previous work (Zhang and Neelamegham, 2002). Specifically, instead of solving a series of complex partial differential equations to calculate the number of cell–substrate collisions as in the previous paper, we demonstrate that nearly identical results can be obtained by using a simpler trajectory/collision-analysis approach. This simplification leads to reduction in model computational time by $\sim$ 50 times. Depending on the choice of parameters, it now takes $\sim$ 10–15 s to simulate a 10-min flow chamber run on a 366-MHz Pentium PC. The new version also eliminates some of the finite-difference approximations that were present in the previous work. Finally, while the previous paper only considered cell rolling and firm-arrest, we have included cell transmigration in the current version. We feel that this is important since leukocyte transmigration is observed in studies where the substrate is composed of human umbilical vein endothelial cells (HUVEC) (Tsang et al., 1997). Rapid cell transmigration may also reduce the contribution of secondary cell–cell capture in adhesion studies. Overall, we anticipate that these model changes and simplifications along with the availability of the code in public domain (at the journal website and at www.eng.buffalo.edu/~neel/pplate) will appeal to biological and immunological laboratories (Zhang and Neelamegham, 2003).

2. Data analysis methodology

The parallel-plate flow chamber consists of two parallel plates of length L separated by a distance $2b$ (Fig. 1). In this schematic, the origin of the (x,y) axis is set at the bottom left-hand corner. The bottom plate of the chamber, corresponding to $y=0$, bears a substrate composed of either ligand-bearing cells or isolated adhesion molecules. In typical experiments, a syringe pump draws a dilute cell suspension into this device at a constant flow rate Q in the x-direction. The wall shear rate (γ_w) at the bottom substrate is related to the flow rate, chamber height, and flow section width (w) by the relation $\gamma_w = 3Q/2b^2w$. The wall shear stress τ_w for a Newtonian fluid with viscosity μ is then defined as $\tau_w = \mu\gamma_w$.

2.1. Cell trajectory

Cells entering the flow chamber are modeled to be spheres of radius a with microvilli protrusions of length λ. These cells both settle onto the bottom substrate due to gravity at a velocity v_{set} and simultaneously convect in the free stream with velocity u_f (Fig. 1). The settling velocity at any point is given by (Davis and Giddings, 1985):

$$v_{set} \approx \frac{v_{set}^0}{1 + a/(y-a)} \quad (1)$$

Here, the numerator v_{set}^0 is the free settling velocity far from the chamber substrate. It is described by Stokes equation ($v_{set}^0 = 2\Delta\rho g a^2/(9\mu)$) where $\Delta\rho$ is the difference between media and cell density ($\rho_c - \rho_m$). As the cell approaches the substrate, its settling velocity is reduced due to a balance between two opposing

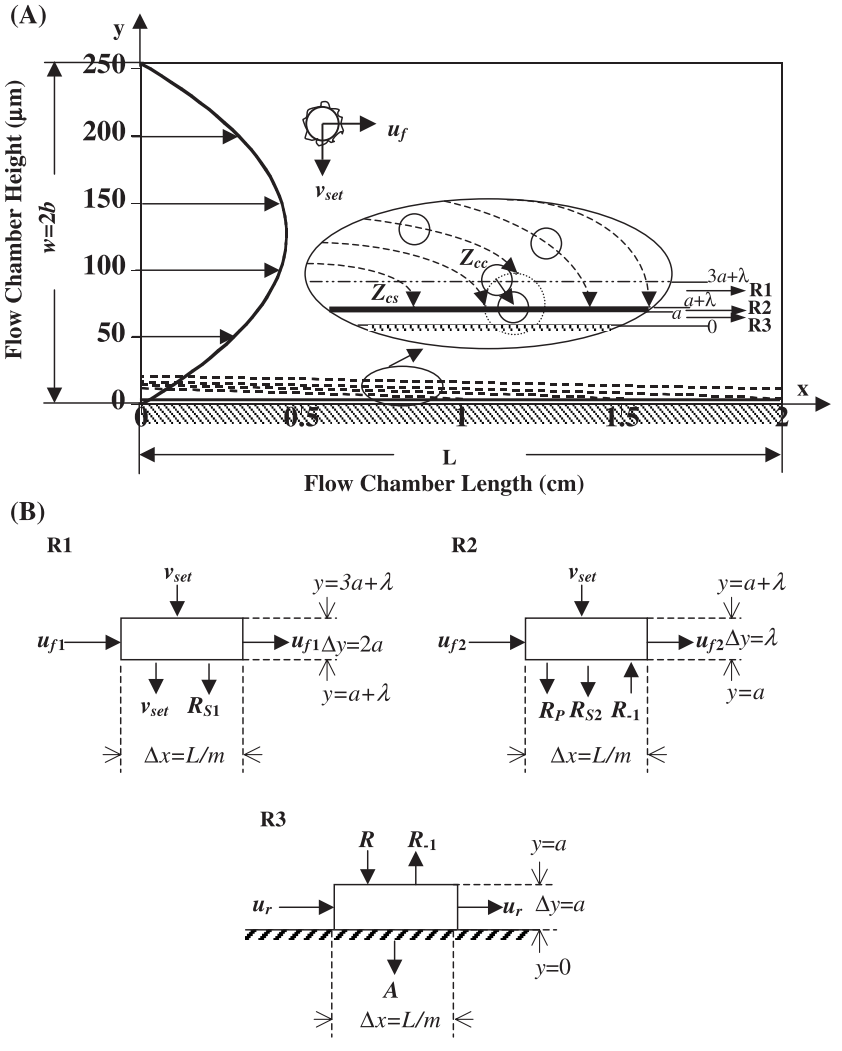

Fig. 1. (A) Flow chamber. Figure depicts a parallel-plate flow chamber of height $2b$ and length L. Cells entering the chamber are modeled as spheres of radius a and microvilli length λ. These cells settle at a velocity v_{set} and convect at a velocity u_f. Dashed lines near the substrate depict cell settling profile under conditions listed in Table 1. As seen, only cells entering close to the substrate make contact with the flow chamber. Expanded insets also depict trajectory of cells. Z_{cs} and Z_{cc} are the frequency of cell–substrate and cell–cell collisions, respectively. (B) Model equations. Model equations are set up for regions R1 ($3a+\lambda>y>a+\lambda$), R2($a+\lambda\geq y\geq a$) and R3 ($y<a$) near the substrate. Cell flux in these three regions is depicted in schematic form. v_{set}, u_f and u_r are used to depict the flux of cells due to cell settling, free-convection and rolling, respectively. R_P and R_{-1} are the rate at which cells either initiate rolling following primary capture, or the rate at which rolling cells are released from the substrate. R_{S1} and R_{S2} depict secondary capture in regions R1 and R2, respectively. R is the total capture rate ($R=R_P+R_{S1}+R_{S2}$). A denotes the firm-arrest rate.

forces: the forces of gravity that drive the particle to the surface, and the lubrication layer between the particle and the substrate that resists this motion. The denominator of Eq. (1) accounts for this lubrication effect. As seen, close to the plate surface when the separation distance ($y-a$) is small, the settling velocity v_{set} tends to 0. Far from the substrate, the denominator is approximately 1.

The convection velocity of the cells in the free stream far from the surface varies quadratically with height from the substrate as described below (Eq. (2a)). Here, u_{max} ($=3Q/(4bw)$) is the maximum con-

vection velocity at the center of the flow chamber. Close to the plate surface (at approximately $y<4a$), the convection velocity is reduced by hydrodynamic wall effects (Goldman et al., 1967). Exact results for u_f at $y<4a$ are well approximated by Eq. (2b):

$$u_f = \frac{u_{max}}{b^2}(2by - y^2) \qquad y \geq 4a \tag{2a}$$

$$u_f = \sim y\gamma_w\left(1 - \frac{5}{16}\left(\frac{a}{y}\right)^3\right) \qquad y < 4a \tag{2b}$$

The equations of settling (Eq. (1)) and convection (either Eq. (2a) or (2b) depending on the y-coordinate) can be combined to yield an equation that describes the (x,y) trajectory of a cell (either Eq. (3a) or (3b)). In this equation, given the coordinate of the cell at any instant say (x_1,y_1), it is possible to determine both the coordinate at which the cell enters the flow chamber (by setting x to zero and solving for y) and the position where it touches the substrate (by setting y to equal $a+\lambda$ and solving for x).

$$x - x_1 = \frac{u_{max}}{b^2 v^0_{set}}\left(\frac{y^3 - y_1^3}{3} + \frac{(a-2b)(y^2 - y_1^2)}{2} + (a^2 - 2ab)(y - y_1) + (a^3 - 2a^2 b) \times \ln\frac{y-a}{y_1 - a}\right) \qquad y \geq 4a \tag{3a}$$

$$x - x_1 = \frac{2u_{max}}{b v^0_{set}}\left(a(y_1 - y) + \frac{(y_1^2 - y^2)}{2} + \frac{5}{16}a^2 \ln\frac{y_1}{y} + \frac{11}{16}a^2 \ln\frac{y_1 - a}{y - a}\right) \qquad y < 4a \tag{3b}$$

The dashed lines in Fig. 1A depict cell trajectories based on Eqs. (3a) and (3b) above at a wall shear stress of 0.2 Pa.

2.2. Rationale for model simplification

Recently, we performed a detailed finite difference analysis of the cell concentration in various regions of the flow chamber (Zhang and Neelamegham, 2002). In that model, the entire volume of the flow chamber ($2b>y>0$) was divided by a two-dimensional 39×11 grid, and the cell concentration in each of the grid elements was monitored. Our calculations revealed that the cell concentration in the free stream above the chamber substrate, that is, at $y>3a+\lambda$, reaches steady state within ~ 10 s of initiation of shear. However, the time to reach steady rolling density is much larger, on the order of several minutes. The difference in times required to reach steady cell densities in these two regions is due to the much larger convective velocity compared to the cell rolling velocity. From a practical perspective, since the free-stream cell concentration reaches steady state rapidly and since typical experimental data is recorded only after the first minute of introduction of cells, time-resolved solution of cell concentration in the free stream ($y>3a+\lambda$) is not necessary. Numerical and computational simplification of the model is hence possible. In other words, detailed solution of cell concentration changes with time is only required for regions close to the substrate (at $y \leq 3a+\lambda$). These regions include Region 1 or R1 ($3a+\lambda>y>a+\lambda$), Region 2 or R2 ($a+\lambda \geq y \geq a$) and Region 3 or R3 ($a>y$) shown in Fig. 1 inset. Each of the three regions is divided into m equal-sized sections along the length of the flow chamber. For the results presented here, m is set to 11. Thus, instead of solving 39×11 partial differential equations as in the previous version (Zhang and Neelamegham, 2002), the current model only requires solution of 3×11 equations. This simplification reduces model computation time by $\sim$ 50-fold.

A brief description of regions R1, R2 and R3 follows. R1 is a region of height $2a$. As shown in Fig. 1B, while convection and settling are prominent features regulating the cell concentration in this region, the capture of cells in R1 by surface-bound cells may also be important. This phenomenon where cell–cell collision results in capture is termed "secondary capture". The rate of secondary capture in R1 is denoted R_{S1} (cell capture/area/time). C_1 denotes the cell concentration in R1 and u_{f1} (equal to u_f at $y=2a+\lambda$) is the mean cell free-stream velocity. R2 is a region of height equal to the cell microvilli length, λ (Fig. 1B). Cells in this region are flowing in the free stream while in contact with the chamber substrate. C_2 and u_{f2} denote the cell concentration and cell free-stream velocity in this region. The majority of cells captured onto the substrate in R2 are recruited via "primary capture"

mechanism. The rate of this process is denoted by R_P (cell capture/area/time). A small fraction of cells in R2 also undergoes secondary capture at a rate R_{S2} (cell capture/area/time). Cells captured from R1 and R2 onto the substrate via both primary and secondary mechanisms initiate rolling (i.e. $R = R_P + R_{S1} + R_{S2}$). In R3, at any instant of time, there is C_r rolling cells per unit area. The rolling velocity is denoted u_r. Some rolling cells may be released into the free stream at a rate denoted R_{-1}. Rolling cells may also undergo firm-arrest in R3 at a rate A (firm-arrest/area/time). C_A (cells/area) denotes the density of firmly adherent cells on the flow chamber substrate at any time. The total number of substrate-bound cells (N_b, cells/area) includes both rolling and adherent cells, that is, $N_b = C_r + C_A$. Methods for computing C_1, C_2, C_r and C_A are discussed below.

2.3. Definition of model frequency and probability parameters

2.3.1. Primary capture frequency

The rate of cell–substrate collision, Z_{cs} (collisions/area/time), equals the rate at which cells settle from R1 into R2. This type of collision controls the cell concentration in R_2, C_2. Mathematically,

$$Z_{cs} = C_1 v_{set}\,|_{at\ y=a+\lambda} \tag{4}$$

A parameter "primary capture frequency", θ_{fr} (unit of length^{-1}) is introduced to provide a measure of cell adhesivity. This parameter is analogous to the adhesion efficiency, which is used to quantify the rate of cell aggregation in suspension (Neelamegham et al., 1997). According to Eq. (5), the primary capture rate R_P increases in proportion to θ_{fr} and C_2. By this definition, the average cell traverses a distance ln(2)/θ_{fr} in region R2 before primary capture (Zhang and Neelamegham, 2002). The average time taken to travel this distance ($t_{1/2}$) is thus ln(2)/($\theta_{fr} u_{f2}$).

$$R_P = \theta_{fr}\lambda u_{f2} C_2 \left(1 - \frac{\pi a^2 N_b}{f_{max}}\right) \tag{5}$$

In the above expression, the term in parentheses is introduced to account for the fact that it is never possible to completely pack the ligand-bearing substrate with rolling cells under real experimental conditions. Thus, at the later time points when a substantial fraction of the substrate area is occupied by rolling and adherent cells, R_P is reduced due to a reduction in free-substrate area available for cell capture. In the above equation, $\pi a^2 N_b$ and f_{max} are the fraction of the substrate area occupied by rolling and adherent cells at any time, and at maximum substrate coverage, respectively. Also, a linear relationship is assumed between capture rate R_P and the substrate area available for cell recruitment. f_{max} is a function of the fluid-flow profile close to the substrate and the receptor and ligand concentration. Because of the effect of local fluid flow, we anticipate that this parameter may be different when cells bind reconstituted purified ligand-bearing substrates in comparison to a monolayer of ligand-bearing cells.

We consider the physical meaning of f_{max}. This parameter can be determined experimentally by performing experiments at high inlet cell concentration and determining the maximum substrate surface area occupied at large times at a given shear rate. Based on such experiments, we estimate f_{max} to be 0.025 when neutrophils bind substrates bearing E-selectin and intercellular adhesion molecule-1 (ICAM-1) cotransfected cells at 0.2 Pa (Zhang and Neelamegham, 2002). The minimum distance of separation between the centers of any two cells of radius r bound on the substrate is one cell diameter ($=2\times r$). This implies that a cell of radius r excludes a region of size ($\pi(2r)^2$) around it. By the same token, a f_{max} value of 0.025 implies that 10% ($=2.5\times 2^2$) of the substrate-area is excluded for the binding of another cell.

2.3.2. Cell–cell capture probability

Cell–cell collisions occur in both R1 and R2. We estimate the number of collisions in each of these regions by applying the concept of "collision sphere". According to this, any cell that is bound on the substrate (either rolling or adherent cell) is surrounded by an imaginary "collision sphere" with radius $=2a$. If the center of any other cell in suspension enters this collision sphere, the distance between the two cells equals one cell diameter, and cell–cell collision is said to occur. Thus, in R1, the frequency of cell–cell collision Z_{cc1} (collisions/area/time) is mathematically expressed as:

$$Z_{cc1} = N_b C_1 \iint_s u_f dA \tag{6}$$

where dA denotes any area element on the collision sphere and u_f is the free-stream velocity at that point. As seen in Fig. 1B, a small portion of the collision sphere also lies in R2. Mathematically, the number of cell–cell collisions in R2, Z_{cc2} (collisions/area/time) can be derived similarly as Z_{cc1} (Eq. (7)). However, since the height of this region is small and the convective velocity is much greater than cell settling velocity, this expression simplifies to:

$$Z_{cc2} = 4a\lambda u_{f2} C_2 N_b \tag{7}$$

The total number of cell–cell collisions (Z_{cc}) taking place in the flow chamber is thus given by the sum of the above, that is, $Z_{cc} = Z_{cc1} + Z_{cc2}$.

In our model, we define a dimensionless parameter "cell–cell capture probability" θ_{cc} to quantify the rate of secondary tethering. By definition, θ_{cc} equals the fraction of cell–cell collisions that result in secondary tethering, and it is always less than 1. The secondary tethering rate (cells captured/area/time) in R1 (R_{S1}) and R2 (R_{S2}), are proportional to both θ_{cc} and the frequency of cell–cell collision in that region (Eqs. (8) and (9)). The f_{max} factor is again introduced in these equations based on arguments above.

$$R_{S1} = \theta_{cc} Z_{cc1}\left(1 - \frac{\pi a^2 N_b}{f_{max}}\right) \tag{8}$$

$$R_{S2} = \theta_{cc} Z_{cc2}\left(1 - \frac{\pi a^2 N_b}{f_{max}}\right) \tag{9}$$

2.3.3. Rolling-release frequency

The rolling-release rate (R_{-1}) is used to quantify the release of cells from rolling back into the free stream. This may occur either when the off-rate of ligands bound on the flow-chamber substrate is high or when the ligand density is sparse. R_{-1} is linearly related to the concentration of rolling cells and the "rolling-release frequency", θ_{rf} (unit of length^{-1}) (Eq. (10)). From a physical standpoint, the average cell can be thought to roll a distance equal to $\ln(2)/\theta_{rf}$ before being released back into the free stream.

$$R_{-1} = \theta_{rf} u_r C_r \tag{10}$$

2.3.4. Firm-arrest frequency

A denotes the adhesion rate (number of cells adhering/area/time). This rate is directly dependent on the number of rolling cells and a parameter "firm-arrest frequency", θ_{ra} (unit of length^{-1}) (Eq. (11)). θ_{ra} is introduced to quantify the frequency with which rolling cells transition to firm-adhesion. Analogous to the primary capture frequency above, $\ln(2)/\theta_{ra}$ is the average distance that the cell rolls before it switches to firm-arrest on the substrate. The time taken for such a transition for an average cell equals $\ln(2)/(\theta_{ra} u_r)$.

$$A = \theta_{ra} u_r C_r \tag{11}$$

2.4. Model mass balance equations

Mass balance equations are written for Regions 1–3 as follows.

2.4.1. Region 1 or R1 ($3a+\lambda > y \geq a+\lambda$)

R1 represents the region where secondary capture, but no primary capture, takes place. The number of settling cells in this region is estimated by applying trajectory equation (Eqs. (3a) and (3b)). According to this equation, given the coordinate at which a cell settles into R1, that is, given $(x_1, 3a+\lambda)$, by retracing the particle trajectory, it is possible to determine the point at which this cell entered the flow chamber, that is, we can determine the entry coordinate $(0, y_2)$, where $y_2 \leq 2b$. It follows that all cells that enter the flow chamber with y-coordinate between y_2 and $3a+\lambda$ settle into R1 in the region between the entrance of the flow chamber and the point $(x_1, 3a+\lambda)$. Mathematically, the number of such collisions (N_{col}, collisions/time) is given by:

$$N_{col}(x_1, 3a+\lambda \mid 0, y_2) = \int_{y=3a+\lambda}^{y_2} C_b u_f w \mathrm{d}y \tag{12}$$

Here, C_b is the inlet cell concentration. Based on the above approach, the number of cells settling into R1 between positions x_1 and $x_1 + \Delta x$ in the flow chamber is given by Eq. (13). Here, SR denotes the settling rate in (cells settling/area/time). Particles entering the flow chamber at $(0, y_2'')$ enter R1 at $(x_1+\Delta x, 3a+\lambda)$. Similarly, particles entering the flow chamber at $(0, y_2')$ enter R1 at $(x_1, 3a+\lambda)$.

$$\mathrm{SR} = \left\lfloor N_{col}(x_1 + \Delta x, 3a+\lambda \mid 0, y_2'') - N_{col}(x_1, 3a+\lambda \mid 0, y_2')\right\rfloor / (w\Delta x) \tag{13}$$

Eq. (14a) below mathematically summarizes the various physical processes controlling the cell concentration in a grid element of R1, located between points x and $x+\Delta x$. The first two terms of this equation quantify cell convection in and out of the grid element. The third and fourth terms denote cell settling rates. Following this is the secondary tethering rate in R1 quantified by R_{S1} (from Eq. (8)). The final term on the right hand side (RHS) represent the time-dependent evolution of cell concentration in R1.

$$2au_{f1}wC_1\,|_{\text{at } x} - 2au_{f1}wC_1\,|_{\text{at } x+\Delta x} + \text{SR}w\Delta x - Z_{cs}w\Delta x - R_{S1}w\Delta x = \frac{d}{dt}(2aC_1w\Delta x) \quad (14a)$$

Introducing parameters $x^*=x/L$, $t^*=(tv^0_{set})/(2b)$, $C_1^*=C_1/C_b$ and $R^*_{S1}=R_{S1}/(C_bv^0_{set})$, we can rewrite Eq. (14a) along with appropriate initial (I.C.) and boundary conditions (B.C.) in dimensionless form:

$$\frac{\partial C_1^*}{\partial t^*} = \frac{b(\text{SR}-Z_{cs})}{av^0_{set}C_b} - \frac{b}{a}R^*_{S1} - \frac{2bu_{f1}}{v^0_{set}L}\frac{\partial C_1^*}{\partial x^*}$$

$$\text{I.C.: } C_1^*=0, \text{ at } t^*=0 \quad (14b)$$

$$\text{B.C.: } C_1^*=1, \text{ at } x^*=0$$

2.4.2. Region 2 or R2 ($a+\lambda \geq y \geq a$)

R2 is the region with height equal to cell microvilli length, λ. All cells in this region are in contact with the substrate. Since several families of leukocyte adhesion molecules including the selectins and their ligands are found localized at the tips of microvilli, primary capture may occur in R2. Eq. (15a) describes the processes regulating the cell concentration in any grid element of R2 located between x and $x+\Delta x$. The first two terms describe the rate of cell convection in and out of R2. The third term denotes the rate of cell settling into R2. Following this are expressions that describe the rate of primary capture (R_P), secondary capture (R_{S2}) and rolling release (R_{-1}). Detailed expressions for R_P, R_{S2} and R_{-1} are described in Eqs. (5), (9) and (10). The final term on the RHS of Eq. (15a) describes the accumulation of cells in R2.

$$u_{f2}\lambda wC_2\,|_{\text{at } x} - u_{f2}\lambda wC_2\,|_{\text{at } x+\Delta x} + Z_{cs}w\Delta x - (R_P+R_{S2}-R_{-1})w\Delta x = \frac{d}{dt}(C_2\lambda w\Delta x) \quad (15a)$$

Eq. (15a) is written in dimensionless form along with initial and boundary conditions as:

$$\frac{\partial C_2^*}{\partial t^*} = -\frac{2bu_{f2}}{v^0_{set}L}\frac{\partial C_2^*}{\partial x^*} - \frac{2b}{\lambda}(R_P^*+R_{S2}^*-R_{-1}^*) + \frac{2bZ_{cs}}{\lambda v^0_{set}C_b}$$

$$\text{I.C.: } C_2^*=0, \text{ at } t^*=0 \quad (15b)$$

$$\text{B.C.: } C_2^*=1, \text{ at } x^*=0$$

where $C_2^*=C_2/C_b$, $R_P^*=R_P/(C_bv^0_{set})$, $R^*_{S2}=R_{S2}/(C_bv^0_{set})$ and $R^*_{-1}=R_{-1}/(C_bv^0_{set})$.

2.4.3. Region 3 or R3 ($a>y>0$)

Cells enter R3 via both primary tethering and secondary capture. Thus, the total rate of cell capture (R) is

$$R = R_P + R_{S1} + R_{S2} \quad (16)$$

Analogous to Eqs. (14a) and (15a), Eq. (17a) describes the overall balance for rolling cell density (C_r, cells/area) in R3. Expressions for R, R_{-1} and A are described in Eqs. (16), (10) and (11), respectively.

$$u_rwC_r\,|_{\text{at } x} - u_rwC_r\,|_{\text{at } x+\Delta x} + (R-R_{-1}-A)w\Delta x = \frac{d}{dt}(C_rw\Delta x) \quad (17a)$$

Upon defining dimensionless parameters $C_r^*=C_r/(aC_b)$, $R^*=R/(C_bv^0_{set})$ and $A^*=A/(C_bv^0_{set})$, Eq. (17a) can be written in dimensionless form along with boundary and initial conditions as:

$$\frac{\partial C_r^*}{\partial t^*} = -\frac{2bu_r}{v^0_{set}L}\frac{\partial C_r^*}{\partial x^*} + \frac{2b}{a}(R^*-R^*_{-1}-A^*)$$

$$\text{I.C.: } C_r^*=0, \text{ at } t^*=0 \quad (17b)$$

$$\text{B.C.: } C_r^*=0, \text{ at } x^*=0$$

The density of adherent cells at any time C_A (cells/area) is based on the cumulative adhesion of cells over the time course of the experiment. At any time t, it is mathematically expressed as:

$$C_A = \sum_{\text{time}=0}^{t}(A-\text{TM}) \quad (18)$$

Here, TM is the transmigration rate (cells transmigrated/area/time), which we define below based on the

average time taken for cell transmigration (t_{TM}, unit of time):

$$TM = \ln(2) \times C_A / t_{TM} \quad (19)$$

The total number of transmigrated cells (C_{TM}, cells/area) at time t is calculated by summing the number of transmigrated cells over each time interval:

$$C_{TM} = \sum_{time=0}^{t} TM \quad (20)$$

3. Model solution and application

The model essentially involves solution of three differential equations (Eqs. (14b), (15b) and (17b)). This is performed by writing a program in FORTRAN and applying the subroutine DDASPG in the IMSL library (Visual Numerics, San Ramon, CA) to solve the equations. DDASPG is a standard subroutine applied to solve sets of first-order differential algebraic equations using the Petzold–Gear BDF method. Documented computer code for this work along with readily usable executable program (PC version) is available from the journal website and http://www.eng.buffalo.edu/~neel/pplate.

The input and output for the program has been tailored for use by typical experimenters. All model parameters along with default simulation values are listed in Table 1. As seen, while the first nine variables can be readily determined for any experimental system, the next three parameters (u_r, f_{max}, t_{TM}) can be determined directly from independent experiments that quantify cell rolling velocity, maximum substrate occupancy and the average transmigration time. The final four variables are frequency and probability parameters (θ_{fr}, θ_{ra}, θ_{rf}, θ_{cc}) that define the biology of the receptor–ligand interactions. These are determined by fitting experimental data on number of rolling, adherent and transmigrated cells with the model as explained below. Although a large number of combinations of the four parameters are possible, we note that in most experimental situations, one or more of the parameters can be set to zero. For example, if secondary capture does not take place or is blocked by specific cell–cell adhesion blocking antibody, θ_{cc} will be set to zero. In the context of studies of leukocyte–endothelium binding, such a scenario takes place when anti-P-selectin glycoprotein ligand-1 (anti-PSGL-1) or anti-L-selectin antibodies are used to block leukocyte–leukocyte interactions (Walcheck et al., 1996). Also, if only cell rolling takes place in the experiment in the absence of firm-arrest, θ_{ra} is zero. This would be expected in studies of selectin-mediated interaction in the absence of integrin/ICAM binding (Puri et al., 1997). Finally, if the release of rolling cells back into the flow is not observed, θ_{rf} may be set to zero.

Overall, our program has two variables (time t and dimensionless position x^*) and four parameters (θ_{fr}, θ_{ra}, θ_{rf} and θ_{cc}). Depending on the nature of the experimental data, the user must choose any two of these six features to vary over a range of values and set all others to fixed values. As an example, consider the case where rolling cell density data is available over the time course of an experiment that examines neutrophil binding to an E-selectin-coated substrate at the center of the flow chamber. Also, suppose that there is no secondary capture or reversible release of

Table 1
Reference values for calculations

Model parameter	Variable, symbol	Reference value
Flow chamber dimensions	Half chamber height, b	1.27×10^{-4} m
	Chamber length, L	0.02 m
Cell properties	Cell radius, a	3.75×10^{-6} m
	Cell microvilli length, λ	0.4×10^{-6} m
	Cell density, ρ_c	1.086×10^{3} kg/m^3
	Inlet cell concentration, C_b	0.2×10^{12} cells/m^3
Media and flow properties	Fluid viscosity, μ	7×10^{-4} kg/m/s
	Media density, ρ_m	1.0233×10^{3} kg/m^3
	Wall shear stress, τ_w	0.2 Pa
Other properties	Rolling velocity, u_r	4.0×10^{-6} m/s
	Fraction of substrate area occupied at maximum cell density, f_{max}	0.025
	Transmigration time, t_{TM}	∞
Frequencies and probability	Primary capture frequency, θ_{fr}	250/m
	Firm-arrest frequency, θ_{ra}	500/m
	Rolling-release frequency, θ_{rf}	0/m
	Cell–cell capture probability, θ_{cc}	0.035

rolling cells under the experimental condition. Now, if the objective of the analysis is to determine θ_{fr} under the experimental conditions, the user may choose to perform model calculation by varying time (from say 60 to 600 s) and θ_{fr} (from say 100 to 500/m) while setting θ_{ra}, θ_{rf} and θ_{cc} to zero, and fixing x^* to 0.5. The output data file, which can be opened using Excel software, would then provide data on the number of rolling and adherent cells with time for a range of θ_{fr} values. By comparing simulation results with real experimental data, θ_{fr} can then be determined for E-selectin-mediated adhesion under the experimental conditions. Knowledge of θ_{fr} can be used to estimate the primary tethering rate, R_p, from Eq. (5) and the time required for tethering ($t_{1/2} = \ln(2)/(\theta_{fr} u_{f2})$). Such experiments along with data fitting can also be performed over a range of shear rates and receptors densities to further define the adhesive features of E-selectin ligand binding under shear.

4. Results

Selected results are presented here with the objective of illustrating the usage of the model. Reference values for the parameters used in these calculations are given in Table 1. This corresponds to the case of neutrophils flowing and adhering on substrates composed of mouse L-cells cotransfected with human E-selectin and ICAM-1. More extensive discussion on the nature of cell adhesion in the flow chamber is provided elsewhere (Zhang and Neelamegham, 2002).

4.1. Cell–cell and cell–substrate collision frequency

The primary objective of this model is to clearly distinguish between the effects of the physical features of the system that control the rate of cell–cell and cell–substrate collision, and the biological factors that influence cellular adhesivity. In Fig. 2, we compare and contrast the relative contributions of cell–cell and cell–substrate collision in the flow chamber at 0.2 Pa. As seen in Fig. 2A, while the number of cell–substrate collisions varies by ~ 20% over 10 min, the number of cell–cell collisions increases continuously with time. Cell–cell collision numbers increase with time since the rate of this event is directly related to the number of substrate-bound cells, N_b, which also increase during the course of the experiment (Eq. (6)). The frequency of cell–cell collision is up to ~ 100 times greater than the frequency of cell–substrate collision. This is because, while cell–substrate collisions are only counted once when the cell enters R2, the same cell may collide multiple times with substrate-bound cells in any given run. In Fig. 2B, it is seen that positional variations in the number of cell–substrate collisions are only observed in the first ~ 20% of the flow chamber while variations in cell–cell collisions are prominent up to $x^* = 0.4$. Overall, the data suggest that secondary tethering is

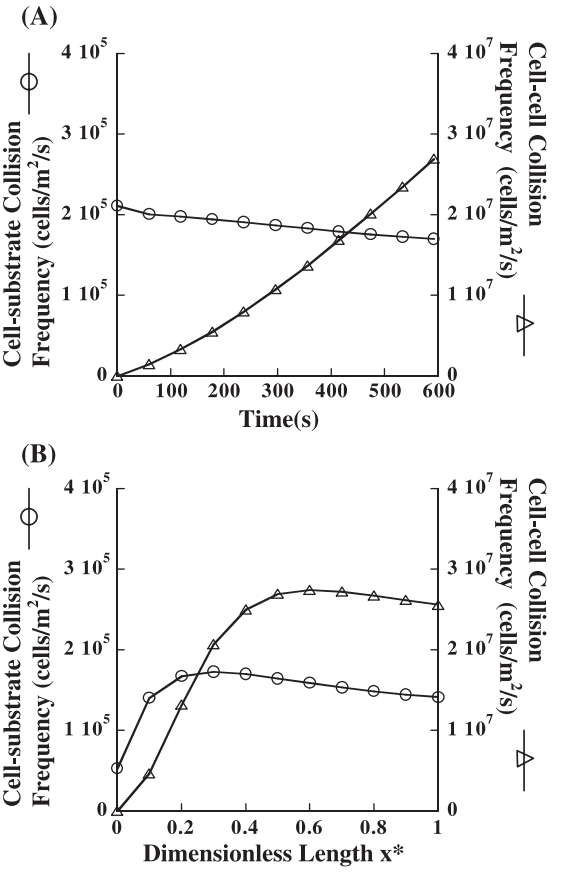

Fig. 2. Collision frequency. Cell–substrate (Z_{cs}, left y-axis) and cell–cell (Z_{cc}, right y-axis) collision frequencies were compared for varying times (panel A) and positions along the length of the flow chamber (panel B). In panel A, the position corresponds to the center of the flow chamber ($x^* = 0.5$), and the data in panel B correspond to the 600-s time point. Model parameters for these calculations are listed in Table 1.

likely to be more important at larger time points and in experiments with higher inlet cell concentrations. This feature may also contribute to variations in cell rolling and adhesion density with position in the flow chamber.

4.2. Rolling and adherent cell density

Fig. 3 illustrates the evolution of rolling and adherent cell density in the flow chamber. As seen, the density of rolling and adherent cells increase with time and steady state is not achieved even at the 600-s time point (Fig. 3A). At this time, ~1% of the substrate area is occupied by the rolling and adherent cells. Also, while positional variations in rolling cell density are more pronounced in the first half of the flow chamber, there is less than a 10% change in cell rolling density between the center and exit of the flow chamber (Fig. 3B). Simulation results, as presented in Fig. 3A, can be used to fit time-resolved experimental rolling and adherent cell density data obtained from flow chamber runs.

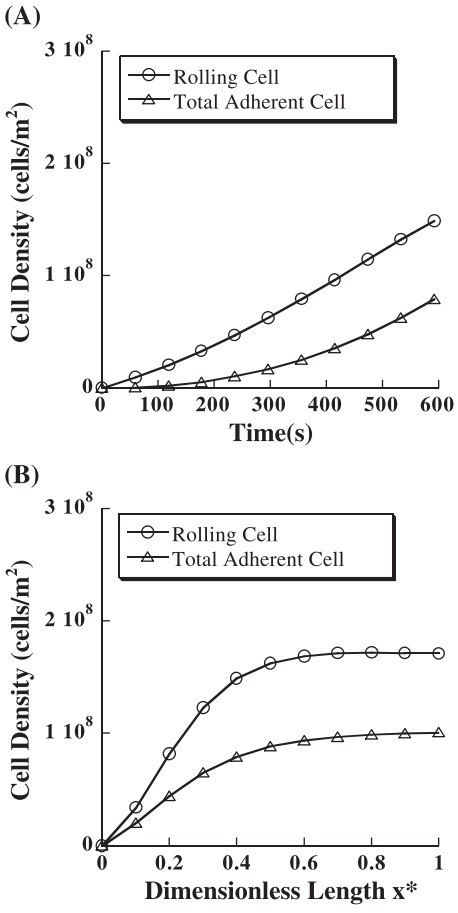

Fig. 3. Cell density. Rolling and adherent cell densities were compared for varying times (panel A) and positions along the length of the flow chamber (panel B). In panel A, the position corresponds to the center of the flow chamber ($x^*=0.5$), and the data in panel B correspond to the 600s time point. Model parameters for these calculations are listed in Table 1.

4.3. Fitting primary capture and firm-arrest frequency to experimental data

In typical experiments, rolling and adherent cell density data are measured at a fixed time for different treatments (e.g. varying antibody treatments or ligand densities). Our data analysis strategy can be applied to estimate the binding frequencies under each of these treatments. For such estimations, a 3-D plot such as Fig. 4A and B can be constructed by providing a range of primary capture (θ_{fr}) and firm-arrest (θ_{ra}) frequencies in a single program run. While Fig. 4A presents data on cell rolling density as a function of θ_{fr} and θ_{ra}, Fig. 4B presents the corresponding data for adherent cell density. Data on cell transmigration are not presented here since the cell transmigration time, t_{TM}, is set to infinite for these simulations. As seen in this figure, since cell capture and adhesion are sequential events, increasing the capture frequency both augments the cell rolling and adhesion density. Similarly, increasing firm-arrest frequency both increases the number of adherent cells and decreases the rolling cell density.

Upon comparison of experimental rolling and adherent cell density data with the plot in Fig. 4A and B, it is possible to estimate the frequency parameters, θ_{fr} and θ_{ra}, for a given experimental condition. Fig. 4C and D presents the data in Fig. 4A and B in an alternate form, as contour plots. In a given example run, if the rolling density is 1.6×10^8 cells/m^2 and adherent density is 0.9×10^8 cells/m^2, the intersection of the dashed lines of equal rolling and adherent cell density in Fig. 4C and D can provide estimates of θ_{fr} (250/m) and θ_{ra} (500/m) for this experiment. This solution can also be derived from the 3-D plots (Fig. 4A and B) as illustrated by the vertical arrows in these panels. Under these conditions, the average cell remains in contact with the substrate (in R2) for 2.97 s ($t_{1/2}=\ln(2)/(\theta_{fr}u_f)$) before tethering, and the

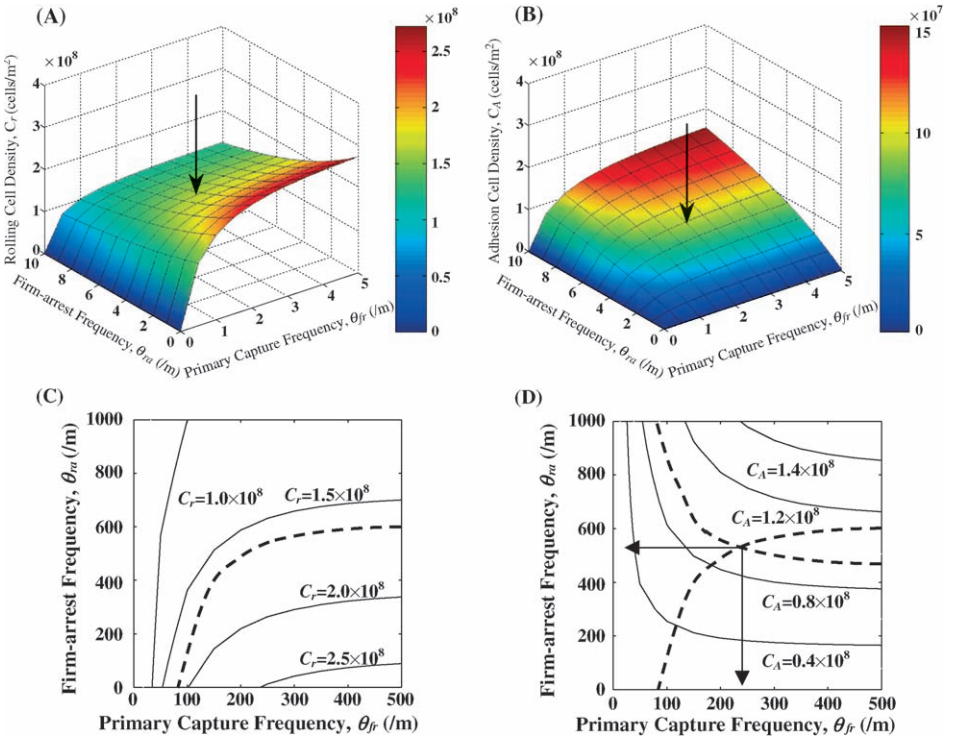

Fig. 4. 3-D and contour plots. The rolling and adherent cell densities were determined at the 600-s time point at the center of the flow chamber for a range of primary capture (θ_{fr}) and firm-arrest (θ_{ra}) frequencies. Values of all other parameters are same as in Table 1. The same set of data is presented both in the form of 3-D plots (panels A and B) and contour plots (panels C and D). In plots C and D, dashed lines depict "experimental" data where the rolling cell density was 1.6×10^8 cells/m^2 (panel C) and the adherent cell density was 0.9×10^8 cells/m^2 (panel D) at the 600-s time point at the center of the flow chamber. As illustrated, the bullet point (θ_{fr} = 250/m and θ_{rf} = 500/m) is common to both the dashed lines in panels C and D. Vertical arrows mark this point (θ_{fr} = 250/m and θ_{rf} = 500/m) in panels A and B. This corresponds to the value of θ_{fr} and θ_{ra} for this experiment.

cell rolls for 346.57 s ($t_{1/2} = \ln(2)/(\theta_{ra} u_r)$) before transitioning to firm-arrest.

5. Discussion

In the current manuscript, we have discussed a strategy to quantify cell adhesion rates in the flow chamber in terms of frequency and probability parameters. These parameters are independent of each other and they aim to describe the average behavior of the cell. They are introduced with the objective of quantifying the biological adhesivity of the cells independent of the physical features of the system. Features that influence the adhesion frequency and probability parameters include the number of receptors and ligands, their affinity, topography, activation levels and their response to applied fluid forces. Of the parameters, the *primary capture frequency* is a measure of the ability of cell adhesion molecules to capture cells from the free stream onto the substrate to initiate rolling. Thus, in typical studies of leukocyte–endothelium binding (Puri et al., 1997), this parameter is a measure of the function of adhesion molecules belonging to the selectin family. Similarly, *firm-arrest frequency* is a measure of the rates at which rolling cells transition to firm-arrest. This is thus a measure of the adhesivity of the integrins and ICAMs, along with the rate at which cells are activated by chemokines expressed on the activated endothelium. The parameter *cell–cell capture probability* is also introduced to distinguish between primary and secondary tethering rates. *Rolling-release frequency* accounts for the release of cells from rolling back into the free stream.

A list of the physical features that affect cell adhesion rates in the flow chamber are provided in Table 1. All of these parameters influence the rolling or adherent cell densities. Of these, the cell and media properties influence the rate of cell settling (Eq. (1)). Together with the applied shear rate, these properties control the trajectory of cells. Among these parameters, we note that the difference between cell and media density ($\rho_c - \rho_m$), the cell size (a) and the microvilli length (λ) are likely to be important in controlling the rate of cell–substrate collision. Since these features vary among various cell types, the pattern of cell rolling and adhesion may also vary in studies that compare the binding function of two different cell types (e.g. neutrophils versus monocytes) to identical substrates, even if the adhesion molecules involved are identical. The contribution of secondary capture to cell adhesion is also dependent on the rate of primary capture, the transmigration time and the inlet cell concentration. By quantifying secondary capture in terms of θ_{cc}, the current analysis methodology allows us to identify the effects of secondary capture independent of the features that affect primary capture and transmigration rates. The model can handle phenomena like cell skipping if a nonzero value is provided for the rolling-release frequency (θ_{rf}). Thus, while there is capture of cells onto the flow chamber via the primary capture frequency (θ_{fr}), there is also simultaneous release of the cells via θ_{rf}.

The objective of the model is to infer the effects of different conditions/treatments on receptor–ligand or cellular adhesivity under fluid shear. Such treatments may include assessment of the effect of adhesion molecule mutations or studies with blocking antibodies. This goal is achieved by fitting experimental data by varying model parameters, especially primary capture and firm-arrest frequency. Once these parameters are determined, it is possible to further analyze these parameters to determine molecular rate constants as discussed elsewhere (Zhang and Neelamegham, 2002).

It is important to note the differences between the practical application of the flow chamber and theoretical assumptions made here. An important consideration is the flow pattern at the entrance and exit of the device. While we assume that the flow is fully developed at the entrance and exit of the flow chamber, this is not the case in real experiments where the flow is typically not at steady state in these regions. Cell concentration determination in these regions is also often difficult due to flow abnormalities. We note, however, that this is not a flaw in the model and such flow effects are likely to influence each experimental treatment in a systematic manner. Thus, regardless of these edge effects, fitting the data for a range of treatments at a fixed point (say the center of the flow chamber) will still provide a measure of the biological adhesivity of cells.

We have recently provided partial validation of a more computationally intensive version of this model (Zhang and Neelamegham, 2002). For this validation, experiments were performed where the rolling, activation and firm-arrest of isolated human blood neutrophils was studied on E-selectin- and ICAM-1-bearing substrates. In the previous work, experimental data fit the mathematical model well over a range of inlet cell concentrations and shear rates. While we have not presented similar validation in the current paper, we wish to state that this verification has been performed with the current version also (data not shown). Overall, the work presented here is consistent with the previous work.

In summary, we present a general data analysis methodology that can be used to analyze cell adhesion data in the parallel-plate flow chamber. While our interest is in studies of cell adhesion in the context of vascular inflammation, we note that this analysis strategy may also be applied to studies of tumor cell metastasis, neutrophil-platelet binding, or platelet thrombosis in models of vascular injury. Similar approaches can also be extended to other flow chambers with alternate geometries.

Acknowledgements

We acknowledge grant support from the Whitaker Foundation and the NIH (HL63014).

References

Alon, R., Hammer, D.A., Springer, T.A., 1995. Lifetime of the P-selectin–carbohydrate bond and its response to tensile force in hydrodynamic flow. Nature 374, 539–542.

Davis, J.M., Giddings, J.C., 1985. Influence of wall-retarded transport of retention and plate height in field-flow fractionation. Sep. Sci. Technol. 20, 699–724.

Felding-Habermann, B., Habermann, R., Saldivar, E., Ruggeri, Z.M., 1996. Role of beta3 integrins in melanoma cell adhesion to activated platelets under flow. J. Biol. Chem. 271, 5892–5900.

Goldman, A.J., Cox, R.G., Brenner, H., 1967. Slow viscous motion of a sphere parallel to a plane wall: II. Couette flow. Chem. Eng. Sci. 20, 653–660.

Gopalan, P.K., Smith, C.W., Lu, H., Berg, E.L., McIntire, L.V., Simon, S.I., 1997. Neutrophil CD18-dependent arrest on intercellular adhesion molecule 1 (ICAM-1) in shear flow can be activated through L-selectin. J. Immunol. 158, 367–375.

Kroll, M.H., Hellums, J.D., McIntire, L.V., Schafer, A.I., Moake, J.L., 1996. Platelets and shear stress. Blood 88, 1525–1541.

Munn, L.L., Melder, R.J., Jain, R.K., 1994. Analysis of cell flux in the parallel plate flow chamber: implications for cell capture studies. Biophys. J. 67, 889–895.

Neelamegham, S., Taylor, A.D., Hellums, J.D., Dembo, M., Smith, C.W., Simon, S.I., 1997. Modeling the reversible kinetics of neutrophil aggregation under hydrodynamic shear. Biophys. J. 72, 1527–1540.

Puri, K.D., Finger, E.B., Springer, T.A., 1997. The faster kinetics of L-selectin than of E-selectin and P-selectin rolling at comparable binding strength. J. Immunol. 158, 405–413.

Tsang, Y.T., Neelamegham, S., Hu, Y., Berg, E.L., Burns, A.R., Smith, C.W., Simon, S.I., 1997. Synergy between L-selectin signaling and chemotactic activation during neutrophil adhesion and transmigration. J. Immunol. 159, 4566–4577.

Walcheck, B., Kahn, J., Fisher, J.M., Wang, B.B., Fisk, R.S., Payan, D.G., Feehan, C., Betageri, R., Darlak, K., Spatola, A.F., Kishimoto, T.K., 1996. Neutrophil rolling altered by inhibition of L-selectin shedding in vitro. Nature 380, 720–723.

Zhang, Y., Neelamegham, S., 2002. Estimating the efficiency of cell capture and arrest in flow chambers: study of neutrophil binding via E-selectin and ICAM-1. Biophys. J. 83, 1934–1952.

Zhang, Y., Neelamegham, S., 2003. PPLATE: a computer program for analysis of parallel plate flow chamber experimental data. J. Immunol. Methods (in press).